

Proceeding Paper

Surface Treatments on Additively Manufactured Ti6Al4V Parts for the Formation of Photocatalytic Nanostructured Surfaces with Antibacterial Properties [†]

Ramón Arcas ^{*}, Lucía Martín, Sales Ibiza, Olga Jordá, Francisco Bosch and Ana Valero-Gómez ^{*}

AIDIMME, Instituto Tecnológico Metalmecánico, Mueblee, Madera, Embalaje y Afines, 46980 Paterna, Spain; lmartin@aidimme.es (L.M.); mibiza@aidimme.es (S.I.); ojorda@aidimme.es (O.J.); fbosch@aidimme.es (F.B.)

^{*} Correspondence: rarcas@aidimme.es (R.A.); avalero@aidimme.es (A.V.-G.)

[†] Presented at the 20th International Conference on Advanced Nanomaterials, Aveiro, Portugal, 24–26 July 2023.

Abstract: Since the emergence of the SARS CoV2 virus, viral and antibacterial disinfection systems have become a global necessity, as well as their effective control and removal. In this context, the improvement of photocatalytic systems for the elimination of microorganisms may play a fundamental role. In this work, a photocatalytic disinfection system was developed and evaluated, based on additively manufactured Ti6Al4V parts using near-visible UV light. Several electrochemical and/or thermal treatments were optimized to obtain different nanostructured morphologies. The results show the effectiveness of the photocatalytic effect (ΔR) on *E. coli* bacteria on different Ti6Al4V modified surfaces, reaching ΔR values between 0.4 and 2.4.

Keywords: additive manufacturing; Ti6Al4V; surface modification; photocatalysis; antibacterial disinfection

1. Introduction

Additive manufacturing (AM) technologies can produce new possibilities in the design and free configuration of novel materials. The main added value of these technologies lies in their versatility, as it allows different parameters related to the 3D printed device to be adjusted, such as geometry, porosity and size [1].

In recent years, titanium and its alloys have positioned themselves as an excellent material for high added-value applications requiring high chemical and mechanical resistance, high stability and low toxicity. In particular, the Ti6Al4V alloy stands out for its high resistance to corrosion and fatigue tests [2,3].

The anodizing process generates nanostructured TiO₂ surfaces that modify the morphology and photocatalytic activity of the electrodes [4]. This process confers unique functional properties, increasing its performance in sectors where AM Ti6Al4V may be of interest, such as sensors [5], lithium-ion batteries [6], hydrogen generation [7], solar cells [8], pollutant degradation by photoelectrocatalysis and electrocatalysis [9,10] or antibacterial surfaces [11]. More specifically, anodizing could be used as treatment to obtain photocatalytic (PC) surfaces that form part of the filters against air pollution in places where the quality of air must be ensured, such as in hospitals. In these places, pollution is complex due to the diversity of activities carried out, the size of the population served and the airborne microorganisms such as bacteria, viruses and others [12]. In recent decades, the application of PC processes for indoor air pollution control has received considerable attention due to the high potential to kill and prevent the growth of microorganisms. And while its use for water purification is well established, its application for large-scale air purification is practically non-existent [13,14]. Recently, some review articles have highlighted the advances on the development of novel materials or surface treatments that can be used for photocatalytic air purification [15,16].



Citation: Arcas, R.; Martín, L.; Ibiza, S.; Jordá, O.; Bosch, F.; Valero-Gómez, A. Surface Treatments on Additively Manufactured Ti6Al4V Parts for the Formation of Photocatalytic Nanostructured Surfaces with Antibacterial Properties. *Mater. Proc.* **2023**, *11*, 4. <https://doi.org/10.3390/materproc2022011004>

Academic Editor: Elby Titus

Published: 27 October 2023



Copyright: © 2023 by the authors. Licensee MDPI, Basel, Switzerland. This article is an open access article distributed under the terms and conditions of the Creative Commons Attribution (CC BY) license (<https://creativecommons.org/licenses/by/4.0/>).

Microbial protection, nanotechnology and additive manufacturing are the three axes on which this article focuses, with the aim of providing technological solutions for the creation of safer environments. Thus, new bactericidal surfaces were obtained through the creation of nanostructured TiO₂ photocatalysts by combining electrochemical and thermal surface modification techniques based on anodizing on titanium parts.

2. Materials and Methods

2.1. Fabrication of Metal Parts

Powder Bed Fusion–Laser Beam (PBF-LB) technology was employed to manufacture the metal parts. In this case, solid cylindrical samples with a radius of 12 mm and thickness of 2 mm were manufactured. They also have an additional longer and narrower cylinder to facilitate electrical contact. The powder employed had a particle size distribution in the range of 15–53 µm.

2.2. Surface Modification Treatment

2.2.1. Constant Potential Anodizing

For the electrochemical oxidation or anodizing process, a commercial rectifier (RKVAN from RECMAC S.A., Madrid, Spain) was employed. In this case, the anodizing process was performed in a single compartment cell using a platinum electrode disk as a counter electrode and the Ti6Al4V electrode as a working electrode. The process was performed at room temperature in an ethylene glycol-based electrolyte containing 0.3% NH₄F and 10% deionized water. To carry out the growth of the nanotubes, a three-step protocol was developed. In the first step, a degreasing of the electrodes was carried out by ultrasound in which the electrodes were subjected to treatment for 10 min first in ethanol and then in water. In the second stage, a constant potential of 60 V was passed over the electrode for 4000 s. Finally, once the electrochemical treatment was finished, the electrodes were subjected to a heat treatment in an air atmosphere at 450 °C for 2 h with a heating rate of 300 °C/h. Samples prepared by this procedure are identified as CP.

2.2.2. Pulsed Wave Potential Anodizing

A procedure similar to the constant potential one was used to prepare samples by a pulsed wave potential. In this case, the applied potential was cycled to two different potentials (60 V and 0 V); in the first one, the growth of the nanotubes occurs and in the second one, the sample goes into a resting state. The pulse time for each potential was set at 40 ms and 10 ms in each case and the total process time was optimized for 15 min. Therefore, the samples labeled PP were prepared.

2.2.3. Thermal Treatment

The heat treatments applied for the preparation of these samples were performed in a tube furnace Nabertherm RSH 120/500/13 and consisted of two consecutive thermal treatments (TT). Initially, the first TT was performed at 450 °C in an uncontrolled air atmosphere, which oxidizes part of the surface to the crystalline structure of TiO₂ anatase. The sample is then heat-treated again at 800 °C in an Ar atmosphere (inlet flow rate). With this last treatment, the aim is to reduce the TiO₂ formed to Ti₃₊ species, which involves the formation of oxygen vacancies on the surface. Samples prepared by this procedure are identified as TT.

2.3. Photoelectrochemical Measurements

Photoelectrochemical measurements were performed on a PGSTAT302N potentiostat (Metrohm-Autolab, The Netherlands) in a home-made one-compartment, three-electrode configuration photoelectrochemical solar cell (PEC). Aqueous Ag/AgCl (12.5 cm from metrohm) and platinum foil (1 cm², metrohm) constituted the reference and counter electrodes and a solution of 0.1 M sodium hydroxide (NaOH) was selected as the electrolyte. PECs were illuminated using LEDs (Taoyuan electron HK limited) with wavelengths of 385

and 405 nm with a power of 50 W. Current density–voltage measurements were carried out under dark and light conditions at a scan rate of 50 mV/s.

2.4. Antibacterial Activity Determination

The effectiveness of the surface modifications on the antimicrobial photocatalytic effect was performed according to ISO 27447:2019 [17], “Fine ceramics (advanced ceramics, advanced technical ceramics)—Test method for antibacterial activity of semiconducting photocatalytic materials”, which evaluates the antibacterial activity of photocatalytic materials.

Firstly, to analyze the microbiological properties, each test surface was sterilized at 120 °C for 20 min.

Secondly, an *Escherichia coli* CECT 516 preserved in glycerol was reactivated on TSA (tryptone soy agar: casein peptone 15 g/L, soy peptone 5 g/L, NaCl 5 g/L, agar 15 g/L), and incubated in a culture chamber for 24 h at 37 °C. Subsequently, a reactivated culture was taken to prepare the inoculum in 1/500 nutrient medium (meat extract 3 g/L, peptone 10 g/L, NaCl 5g/L) using a sterile inoculating loop. The bacterial concentration was calculated spectrophotometrically. The absorbance was measured by a Cary 60 UV-Vis (Agilent technologies) spectrophotometer at 625 nm until it reached 0.08 OD, equivalent to 10⁸ CFU/mL.

After that, the samples were inoculated with an *E. coli* concentration of 10⁶ cells/mL. A film was then placed over the inoculated parts. The plate containing the samples to be tested in the dark was then wrapped in aluminum foil and placed in the incubation chamber at 37 °C for 15 min. The UV test samples were placed 25 cm below the 405 nm UV lamp and tested for 15 min in a chamber at 25 °C. This testing time was determined based on an initial test carried out at different UV light incidence times.

Microorganisms were recovered from samples in neutralizing broth (peptone 1 g/L, L-histidine HCl 1 g/L, leucine 3 g/L, KH₂PO₄ 3.6 g/L, Na₂HPO₄ 7.20 g/L, NaCl 4.30 g/L) and inoculated onto Tryptone Soy Agar (TSA; Scharlau) plates. After the testing, the pieces were washed together with their respective film in a neutralizing agent, NA. They were then vortexed for 2 min and diluted in phosphate buffer and seeded into Petri dishes, which were then incubated for 24 h at 37 °C.

Finally, after the incubation time, the viable number of *E. coli* cells was measured to calculate the photocatalytic antibacterial effect. For this purpose, the logarithmic difference (ΔR) between the results of the samples tested in the dark and the results of the samples irradiated with UV light were compared.

$$\Delta R = \log\left(\frac{B_L}{C_L}\right) - \log\left(\frac{B_D}{C_D}\right) \quad (1)$$

where:

ΔR is the photocatalytic antibacterial activity with UV irradiation.

B_L is the mean viable number of bacteria in untreated samples after UV irradiation.

C_L is the mean viable number of bacteria in treated samples after UV irradiation.

B_D is the mean viable number of bacteria in untreated samples after incubation in the dark.

C_D is the mean viable number of bacteria in treated samples after incubation in the dark.

3. Results

A powder bed fusion technology melted by laser radiation (PBF-LB) was used to fabricate solid pieces with a lollipop-type structure. These structures were 12 cm in diameter and 2 mm wide and were composed of a Ti6Al4V alloy. The surface structure and morphology of the manufactured parts were studied by high-resolution field emission scanning electron microscopy (HRFESEM). Figure S1 shows the surface micrograph of the samples fabricated by PBF-LB. The micrograph shows a microporous surface due to the presence of the unmelted metal powder.

3.1. Surface Modifications

The controlled surface modification of these Ti6Al4V surfaces fabricated with PBF-LB technologies can provide new catalytic surfaces composed of TiO_x systems with a high surface area [5]. For this reason, three different structures obtained from the optimization of three different surface treatments were investigated. Two routes consisted of electrochemical anodizing of the surface, one at a constant potential (CP) and the other with a pulsed potential (PP), followed by a thermal treatment in an air atmosphere. These two treatments aim to achieve TiO_2 structures with an anatase-like structure [18]. A third route consisted of oxidation–reduction through thermal treatments (TT). An initial thermal treatment in an air atmosphere followed by a reducing thermal treatment in an Ar atmosphere were used to develop TiO_2 structures containing oxygen vacancies [19].

Figure 1 shows the micrographs of the structures obtained on the Ti6Al4V surface after each surface modification process. It can be seen how each surface modification leads to a different nanostructured surface. In the first case, samples prepared by PP showed a homogeneous nanoporous structure in which the size of the pores was around 100 nm. On the other hand, samples prepared at a constant potential produced a pore elongation leading to the appearance of nanotube-like structures. As for the samples produced by TT, the nanostructured flake-like surface is noteworthy.

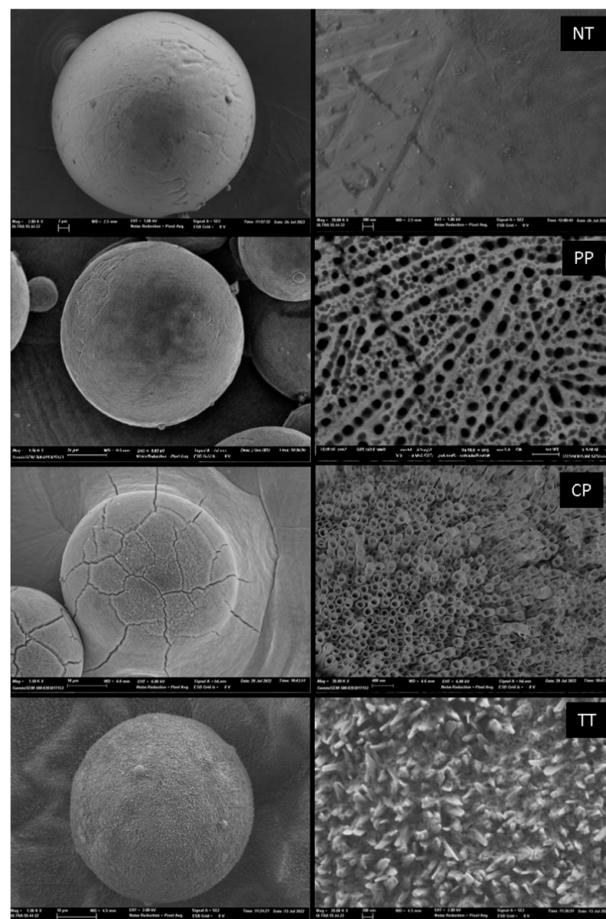


Figure 1. Micrographs at 2000 \times and 20,000 \times of Ti6Al4V parts manufactured by PBF-LB with different surface treatments. NT—no treatment; PP—pulsed potential anodizing; CP—constant potential anodizing; and TT—thermal treatment.

3.2. Photoelectrocatalytic Properties

The photoelectrocatalytic properties of each surface were studied by cyclic voltammetry under light and dark conditions (see Table S1 in supporting information). In order to test the effect of the treatment on the electronic properties of the generated TiO₂ layer, measurements were carried out using different wavelength lamps at 365 nm, 385 nm, 405 nm and 440 nm.

As shown in Table S1, the highest photoelectrocatalytic response occurred at a wavelength of 365 nm for both the untreated sample and the TT sample. However, for the samples prepared by electrochemical anodization, the maximum response was obtained at longer wavelengths: 385 nm for the sample prepared by CP and 405 nm for the sample prepared by PP. This indicates a band gap shift due to the anodization process, which has been observed in previous publications.

The cyclic voltammetry measurements presented in Table S1 show a large capacitance related to two oxidation peaks at 0.5 V and 1.5 V vs. RHE that may be a consequence of the redox processes related to either the formation of TiO₂ structures or to the vanadium present in these samples. However, their influence on the photoelectrocatalytic properties remains beyond the scope of the present work. In order to eliminate part of the capacitive current and determine whether all the current obtained was generated by the effect of light, pulsed light chronoamperometry measurements were carried out. The results obtained are represented in Figure 2 for each surface treatment. The figure shows an improvement in the photocatalytic properties of the modified parts with respect to the untreated surface (NT). Furthermore, the highest photocatalytic capacity was obtained in the sample treated by TT, whose photocurrent values exceeded the rest of the samples by an order of magnitude at 385 nm. With a longer wavelength lamp (405 nm), the photoelectrocatalytic properties of the TT sample decreased and its response was doubled compared to the PP sample.

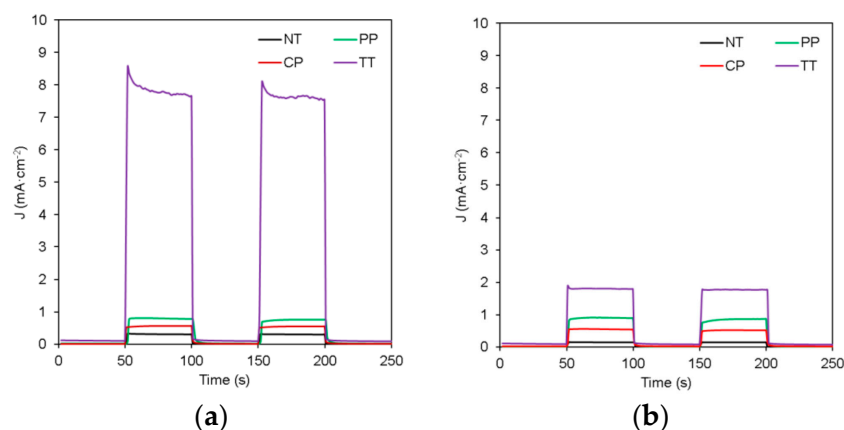


Figure 2. Pulsed light chronoamperometry measurements of surface-modified PBF-LB prepared Ti6Al4V samples. Light excitation: (a) 385 nm (b) 405 nm. Measurements conditions: NaOH 0.1 M, applied voltage 1.6 V vs. RHE.

To further investigate how the surface of the fabricated parts affects the photocatalytic properties, impedance spectroscopy measurements were carried out. The measurements were performed under open-circuit conditions and for each surface, light and dark conditions were studied. Figure 3 shows the Nyquist and bode plots obtained for each surface modification. Considering the resistance values obtained in the bode plot, a relationship between the resistance and the photocatalytic properties of the sample can be observed. Thus, high resistances, such as the one observed in the non-treated sample, imply a reduction in the photocatalytic properties while lower resistances present a higher photocatalytic performance.

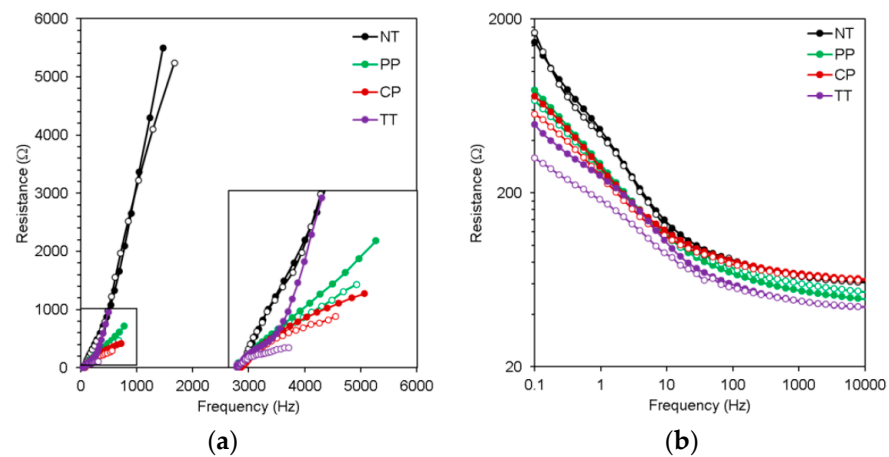
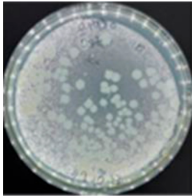
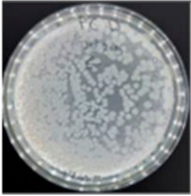
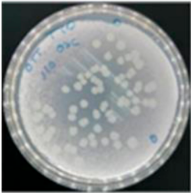
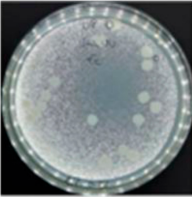
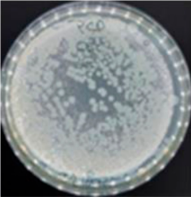
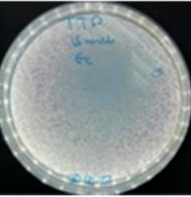


Figure 3. Impedance spectroscopy measurements of surface-modified PBF-LB prepared Ti6Al4V samples. (a) Nyquist plot; (b) bode plot. Measurements conditions: NaOH 0.1 M, open-circuit conditions.

3.3. Antibacterial Photocatalytic Evaluation

The effectiveness of surface modifications on the antibacterial photocatalytic effect was performed according to ISO 27447:2019 [17], which evaluates the antibacterial activity in photocatalytic materials. To carry out the assay, a pseudobiofilm of *Escherichia coli* was inoculated onto the surface of the samples. Once inoculated, the samples were subjected to 15 min with and without light exposure. The antibacterial activity results (Table 1) follow the same trend observed for the photocatalytic properties. Thus, the effectiveness of the photocatalytic properties of TiO₂ in enhancing antibacterial properties was demonstrated. In fact, the photocatalytic effect in the surface-modified samples reduced the proliferation of the bacteria by preventing their growth on the Ti6Al4V surface.

Table 1. *E. coli* colonies and logarithmic colony reduction due to the photocatalytic properties of surface-modified PBF-LB Ti6Al4V samples.

	PP	CP	TT
No Light			
Near UV-Light			
ΔR	1.2	0.4	2.4

4. Conclusions

Photocatalytic devices with antibacterial activity were designed from Ti6Al4V parts combining structures by metal additive manufacturing technologies, such as laser powder bed fusion process (PBF-LB) with two anodizing processes (PP and CP) and two different thermal treatments (Air and Ar). In this way, until three methodologies have been optimized to modify Ti surfaces through the formation of different TiO₂ structures, we have generated three surface modification routes with different nanometric morphology

(nanoporous (PP), nanotubular (CP) and with nanometric flakes (TT)) and different photocatalytic properties. Moreover, these metallic structures were accurately validated in the proliferation of *E. coli*, showing a relationship between the photocatalytic properties and the disinfection of its surface, reaching ΔR values of 0.4 (CP), 1.2 (PP) and 2.4 (TT). In general, the TT methodology showed the best performance in photocatalytic response as well as in antibacterial activity, followed by PP and finally CP, for all wavelengths studied.

Supplementary Materials: The following supporting information can be downloaded at: <https://www.mdpi.com/article/10.3390/materproc2022011004/s1>, Figure S1: Micrograph at $200\times$ of the Ti6Al4V parts manufactured by PBF-LB. Microporosity is due to the presence of unmelted metallic powder; Table S1: Cyclic voltammetry measurements under dark (black) and light conditions of surface-modified PBF-LB manufactured Ti6Al4V samples. Different photoelectrocatalytic responses under illumination with different wavelengths were observed.

Author Contributions: R.A.: Conceptualization, Data curation, Funding acquisition, Investigation, Methodology, Supervision and Writing—reviewing and editing. A.V.-G.: Conceptualization, Data curation, Investigation, Methodology, Writing—reviewing and editing and Project administration. L.M.: Investigation and Methodology. F.B.: Conceptualization, Funding acquisition, Project administration and Writing—reviewing and editing. O.J.: Resources and Methodology. S.I.: Data curation, Investigation and Methodology. All authors have read and agreed to the published version of the manuscript.

Funding: The authors would like to thank the Instituto Valenciano de Competitividad Empresarial (IVACE) from Spain (IMDEEA/2021/13, IMDEEA/2022/52) for its financial support. The Electron Microscopy Service of the UPV (Universitat Politècnica de València) is gratefully acknowledged for their help with the HRFSEM.

Institutional Review Board Statement: Not applicable.

Informed Consent Statement: Not applicable.

Data Availability Statement: The data presented in this study are available in <https://www.aidimme.es/proyectos/detalles.asp?id=30762> and <https://www.aidimme.es/proyectos/detalles.asp?id=32891>.

Conflicts of Interest: The authors declare no conflict of interest.

References

1. Browne, M.P.; Redondo, E.; Pumera, M. 3D Printing for Electrochemical Energy Applications. *Chem. Rev.* **2020**, *120*, 2783–2810. [[CrossRef](#)] [[PubMed](#)]
2. ASM Handbook Committee. *Properties and Selection: Nonferrous Alloys and Special-Purpose Materials*; ASM International: Materials Park, OH, USA, 1990. [[CrossRef](#)]
3. Agius, D.; Kourousis, K.I.; Wallbrink, C. A Review of the As-Built SLM Ti-6Al-4V Mechanical Properties towards Achieving Fatigue Resistant Designs. *Metals* **2018**, *8*, 75. [[CrossRef](#)]
4. Roy, P.; Berger, S.; Schmuki, P. TiO₂ Nanotubes: Synthesis and Applications. *Angew. Chem. Int. Ed.* **2011**, *50*, 2904–2939. [[CrossRef](#)] [[PubMed](#)]
5. Lamberti, A.; Virga, A.; Chiadò, A.; Chiodoni, A.; Bejtka, K.; Rivolo, P.; Giorgis, F. Ultrasensitive Ag-coated TiO₂ nanotube arrays for flexible SERS-based optofluidic devices. *J. Mater. Chem. C* **2015**, *3*, 6868–6875. [[CrossRef](#)]
6. Lamberti, A.; Garino, N.; Sacco, A.; Bianco, S.; Chiodoni, A.; Gerbaldi, C. As-grown vertically aligned amorphous TiO₂ nanotube arrays as high-rate Li-based micro-battery anodes with improved long-term performance. *Electrochim. Acta* **2015**, *151*, 222–229. [[CrossRef](#)]
7. Cui, H.; Zhao, W.; Yang, C.; Yin, H.; Lin, T.; Shan, Y.; Xie, Y.; Gu, H.; Huang, F. Black TiO₂ nanotube arrays for high-efficiency photoelectrochemical water-splitting. *J. Mater. Chem. A* **2014**, *2*, 8612–8616. [[CrossRef](#)]
8. Kuang, D.; Brillet, J.; Chen, P.; Takata, M.; Uchida, S.; Miura, H.; Sumioka, K.; Zakeeruddin, S.M.; Grätzel, M. Application of Highly Ordered TiO₂ Nanotube Arrays in Flexible Dye-Sensitized Solar Cells. *ACS Nano* **2008**, *2*, 1113–1116. [[CrossRef](#)] [[PubMed](#)]
9. Massa, A.; Hernández, S.; Lamberti, A.; Galletti, C.; Russo, N.; Fino, D. Electro-oxidation of phenol over electrodeposited MnOx nanostructures and the role of a TiO₂ nanotubes interlayer. *Appl. Catal. B Environ.* **2017**, *203*, 270–281. [[CrossRef](#)]
10. He, X.; Cai, Y.; Zhang, H.; Liang, C. Photocatalytic degradation of organic pollutants with Ag decorated free-standing TiO₂ nanotube arrays and interface electrochemical response. *J. Mater. Chem.* **2011**, *21*, 475–480. [[CrossRef](#)]
11. Ercan, B.; Taylor, E.; Alpaslan, E.; Webster, T.J. Diameter of titanium nanotubes influences anti-bacterial efficacy. *Nanotechnology* **2011**, *22*, 295102. [[CrossRef](#)] [[PubMed](#)]

12. Baurès, E.; Blanchard, O.; Mercier, F.; Surget, E.; le Cann, P.; Rivier, A.; Gangneux, J.-P.; Florentin, A. Indoor air quality in two French hospitals: Measurement of chemical and microbiological contaminants. *Sci. Total Environ.* **2018**, *642*, 168–179. [[CrossRef](#)] [[PubMed](#)]
13. Kim, J.H.; Seo, G.; Cho, D.-L.; Choi, B.-C.; Kim, J.-B.; Park, H.-J.; Kim, M.-W.; Song, S.-J.; Kim, G.-J.; Kato, S. Development of air purification device through application of thin-film photocatalyst. *Catal. Today* **2006**, *111*, 271–274. [[CrossRef](#)]
14. Lee, H.U.; Park, S.Y.; Lee, S.C.; Seo, J.H.; Son, B.; Kim, H.; Yun, H.J.; Lee, G.W.; Lee, S.M.; Nam, B.; et al. Highly photocatalytic performance of flexible 3 dimensional (3D) ZnO nanocomposite. *Appl. Catal. B Environ.* **2014**, *144*, 83–89. [[CrossRef](#)]
15. Mansoorianfar, M.; Tavoosi, M.; Mozafarinia, R.; Ghasemi, A.; Doostmohammadi, A. Preparation and characterization of TiO₂ nanotube arrays on Ti6Al4V surface for enhancement of cell treatment. *Surf. Coat. Technol.* **2017**, *321*, 409–415. [[CrossRef](#)]
16. Abidi, M.; Hajjaji, A.; Bouzaza, A.; Trablesi, K.; Makhlouf, H.; Rtimi, S.; Assadi, A.A.; Bessais, B. Simultaneous removal of bacteria and volatile organic compounds on Cu₂O-NPs decorated TiO₂ nanotubes: Competition effect and kinetic studies. *J. Photochem. Photobiol. A Chem.* **2020**, *400*, 112722. [[CrossRef](#)]
17. ISO 27447:2009; Fine Ceramics (Advanced Ceramics, Advanced Technical Ceramics) Test Method for Antibacterial Activity of Semiconducting Photocatalytic Materials. International Organization for Standardization (ISO): Geneva, Switzerland, 2009.
18. Ge, M.-Z.; Cao, C.-Y.; Huang, J.-Y.; Li, S.-H.; Zhang, S.-N.; Deng, S.; Li, Q.-S.; Zhang, K.-Q.; Lai, Y.-K. Synthesis, modification, and photo/photoelectrocatalytic degradation applications of TiO₂ nanotube arrays: A review. *Nanotechnol. Rev.* **2016**, *5*, 75–112. [[CrossRef](#)]
19. Wang, G.; Wang, H.; Ling, Y.; Tang, Y.; Yang, X.; Fitzmorris, R.C.; Wang, C.; Zhang, J.Z.; Li, Y. Hydrogen-treated TiO₂ nanowire arrays for photoelectrochemical water splitting. *Nano Lett.* **2011**, *11*, 3026–3033. [[CrossRef](#)] [[PubMed](#)]

Disclaimer/Publisher’s Note: The statements, opinions and data contained in all publications are solely those of the individual author(s) and contributor(s) and not of MDPI and/or the editor(s). MDPI and/or the editor(s) disclaim responsibility for any injury to people or property resulting from any ideas, methods, instructions or products referred to in the content.